Source process and near-source ground motions of the 2005 West Off Fukuoka Prefecture earthquake

Kimiyuki Asano and Tomotaka Iwata

Disaster Prevention Research Institute, Kyoto University, Gokasho, Uji, Kyoto 611-0011, Japan

(Received August 8, 2005; Revised October 4, 2005; Accepted October 12, 2005; Online published January 27, 2006)

A large shallow crustal earthquake occurred at the western off-shore of Fukuoka Prefecture, northern Kyushu, Japan, at 10:53 on March 20, 2005 (JST). Source rupture processes of the mainshock and the largest aftershock on April 20, 2005, are estimated by the kinematic waveform inversion of strong motion seismograms. The rupture of the mainshock started with relatively small slip, and the largest slip was observed at the southeast of the hypocenter. The inverted source models showed that both of the ruptures of the mainshock and the largest aftershock mainly propagated to southeast from the hypocenters, and the rupture area of those events did not overlap each other. Three-dimensional ground motion simulation by the finite difference method considering three-dimensional bedrock structure was also conducted to see the spatial variation of the near-source ground motion of the mainshock. The result of the simulation shows that expected groud motions are relatively large in and arround Genkai Island, Shikanoshima Island, and the center of Fukuoka City compared to the other area because of the rupture heterogeneity and the deep basin structure in Fukuoka City.

Key words: the 2005 West Off Fukuoka Prefecture earthquake, source process, kinematic waveform inversion, strong ground motion simulation.

1. Introduction

At 10:53 on March 20, 2005 (JST), a large shallow crustal earthquake ($M_{\rm JMA}$ 7.0) occurred beneath the Sea of Genkai, western off-shore of Fukuoka Prefecture, northern Kyushu, Japan. Though this earthquake occurred beneath the sea, it brought severe strong ground motions to the near-source region, such as Genkai Island, Shikanoshima Island, and the central district of Fukuoka City. At 06:11 on April 20, 2005, the largest aftershock ($M_{\rm JMA}$ 5.8) occurred just below Shikanoshima Island near the southeastern edge of the fault plane of the mainshock.

The main purpose of this paper is to understand strong motion generation process of these earthquakes. At first, the source process of the 2005 West Off Fukuoka Prefecture earthquake is studied using the strong motion seismograms obtained by Japanese nation-wide strong motion seismograph networks, K-NET (Kinoshita, 1998) and KiK-net (Aoi *et al*., 2001). These networks are installed and operated by the National Research Institute for Earth Science and Disaster Prevention (NIED). The source process of the largest aftershock on April 20, 2005, is also estimated in the same manner. Relationship between the fault rupture of the mainshock and that of the largest aftershock is discussed. Finally, a three-dimensional ground motion simulation using a finite difference method reveals the spatial variation of ground motions in the near-source area.

2. Source Process of the Mainshock

2.1 Methodology

The source rupture process of the mainshock is estimated by the kinematic linear waveform inversion with multiple time windows (Sekiguchi *et al*., 2000). This methodology is originally based on the technique developed by Hartzell and Heaton (1983). The methodology employed here was described in detail by Sekiguchi *et al*. (2000). A planar fault plane model is assumed referring to the aftershock distributions. The length and width of the fault plane are 26 km and 18 km, respectively. According to the moment tensor solution by the F-net (NIED), the strike and dip of the fault plane are assumed to be 122° and 87°, respectively. The rupture starting point is fixed at the hypocenter location (33.75°N, 130.16°E, 14 km) determined by the Institute of Seismology and Volcanology, Faculty of Sciences, Kyushu University (ISV). The fault plane is divided into 117 subfaults of 2 km × 2 km. The temporal slip history at each subfault is expressed by a series of 6 smoothed ramp functions, which has the rise time of 1.0 s, separated by 0.5 s. The rupture front propagation velocity triggering the rupture of the first time window is selected so as to minimize the residual of data fitting. The spatio temporal smoothing to reduce instability or excess of complexity, which reduces the differences among slip amounts close in space and in time, is also included in the analysis following Sekiguchi *et al*. (2000). ABIC approach (Akaike, 1980) is used to select an appropriate strength of the smoothing constraint. The rake angles variation are also limited within ±45° using the non-negative least-squares method (Lawson and Hanson, 1974).

The Green's functions between each subfault and each station are calculated by the discrete wavenumber method

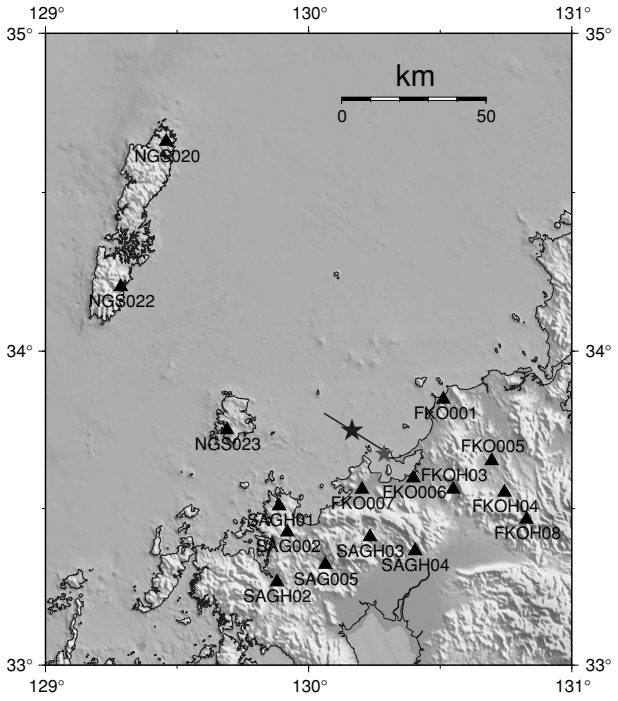

Fig. 1. Map showing studied area. The black and gray stars indicate the epicenters of the mainshock and the largest aftershock, respectively. The solid line shows the projection of the fault plane of the mainshock. Solid triangles indicate the locations of strong motion stations used for the waveform inversion.

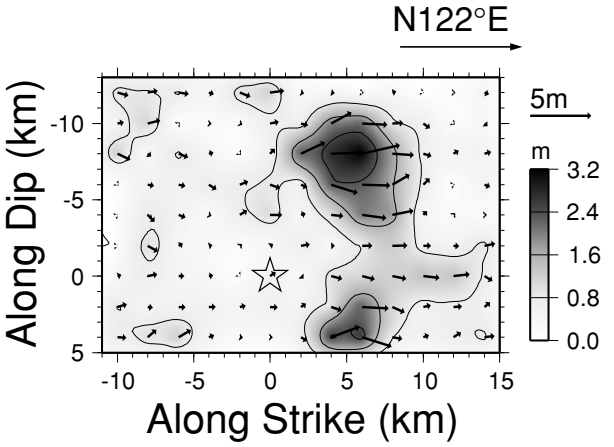

Fig. 2. Final slip distribution of the mainshock estimated from the inversion. The open star indicates the rupture starting point. The allows show the slip vectors of the hanging wall relative to the foot wall. The interval of contours is 0.8 m.

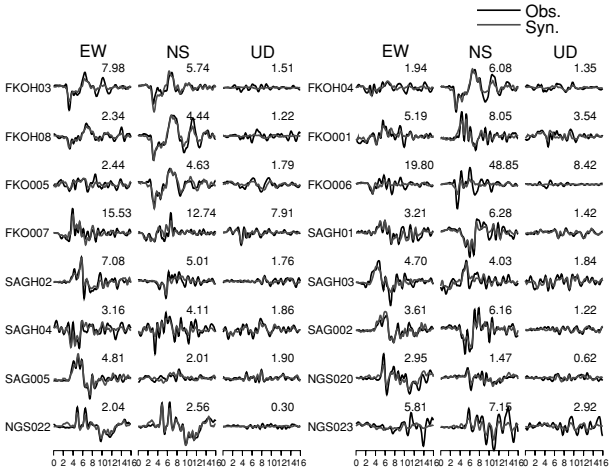

Fig. 3. Comparison between observed (black traces) and synthesized (gray traces) velocity waveforms of the mainshock. The maximum amplitude of each component of observed waveforms are shown above each trace in cm/s. The horizontal axis is time (s).

(Bouchon, 1981) with the reflection and transmission matrix method (Kennett and Kerry, 1979).

Data at nine stations of the K-NET and seven stations of the KiK-net are used for the waveform inversion (see Fig. 1). For the KiK-net stations, uphole seismograph data is used. From among many available stations, stations which have enough quality to retrieve the source process were selected by the visual inspection. Observed digital acceleration data are integrated into the ground velocities in the time domain and bandpass filtered with a Chebyshev filter between 0.05 and 1.0 Hz. We inverted 16 s of the *S*-wave portion from 1 s before the direct *S*-wave arrival. Theoretical Green's functions are also bandpass filtered in the same manner.

2.2 Underground structure model

To calculate the Green's functions, a one-dimensional underground structure model is assumed for each station referring to the underground structure model proposed by Nakamichi and Kawase (2002). They used the underground structure model to evaluate the strong ground motions for a scenario earthquake on the Kego fault in Fukuoka City, so we think this model would be appropriate for the studied area in this paper. Several low-velocity layers for superficial layers at each station are also introduced based on the borehole logging information released by the K-NET and KiK-net. So, the velocity models of the sedimentary part differ slightly from one station to another.

2.3 Result

Figure 2 shows the final slip distribution on the fault surface estimated by the inversion. The rupture front propagation velocity, which triggers the rupture of the first time window, was selected to be 2.1 km/s. This is approximately equal to 60% of the shear-wave velocity at the depth of the rupture, that is a little slower than the average rupture velocity (72%) of shallow crustal earthquakes empirically obtained by Geller (1976). The rupture mainly propagated to the southeastward. The asperity or large slip area with the maximum slip of 3.2 m was observed at southeast of the hypocenter, and relatively smaller slip was observed in the vicinity of the hypocenter. The slip direction is almost pure left-lateral strike slip, which is consistent with the regional stress field in northern Kyushu (Seno, 1999). Figure 3 shows the comparison between the observed and synthesized ground velocities in 0.05–1.0 Hz. The synthesized waveforms match well the observed ones at most stations. We think that the source model obtained here is reliable to represent the source rupture process of this earthquake. However, the large amplitude of velocity pulse in the NS component at Fukuoka (FKO006), which is located inside the Fukuoka basin, could not be reproduced well.

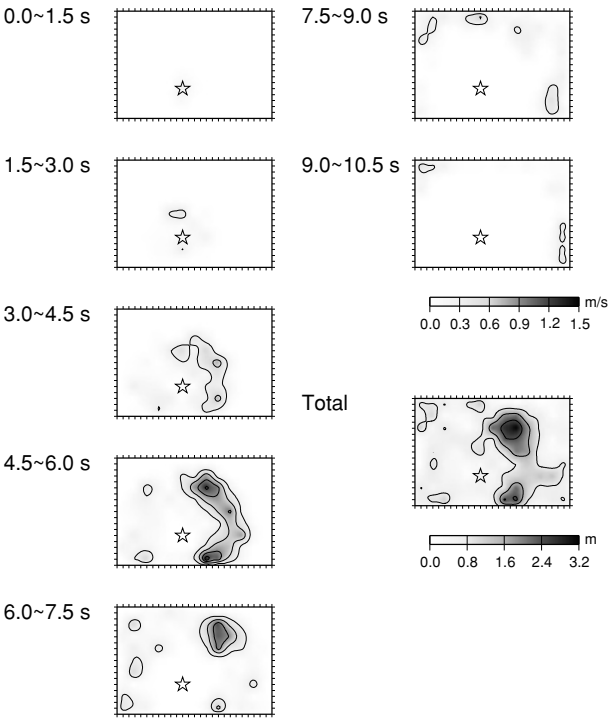

Fig. 4. Snapshots of the temporal rupture progression on the fault at time step of 1.5 s. The contour interval of the slip velocity is 0.3 m/s. The open star indicates the rupture starting point. The figure at bottom right shows the final slip distribution.

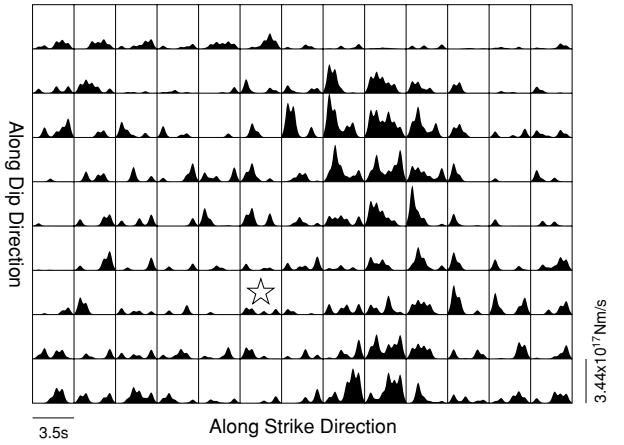

Fig. 5. Moment rate functions of each subfault of the mainshock. The open star indicates the hypocenter.

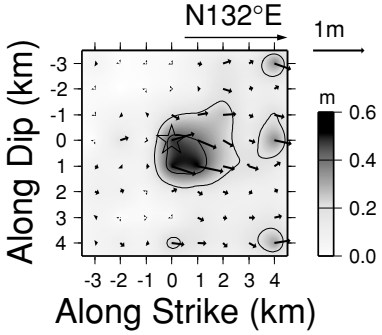

Fig. 6. Final slip distribution of the largest aftershock on April 20, 2005, estimated from the inversion. The open star indicates the rupture starting point. The allows show the slip vectors of the hanging wall relative to the foot wall. The interval of contours is 0.2 m.

Figures 4 and 5 show the temporal rupture progression on the fault. The rupture started from the hypocenter with the small slip velocity, and the entire rupture continued for approximately 10 s. The asperity ruptured at approximately 3.5 s after the initiation of the rupture. The total seismic moment was estimated to be 1.15×10^{19} Nm (M_W6.6). The characteristics of the rupture process of this event mentioned in this section is consistent with the analysis of the initial and main rupture phases by Takenaka *et al*. (2006), in which they determined the rupture time and the location of the main rupture using the onset data of strong motion records. Other studies on the rupture process of this event (Horikawa, 2006; Kobayashi *et al*., 2006; Sekiguchi *et al*., 2006) also show similar results to our source model.

3. Source Process of the Largest Aftershock on April 20, 2005

3.1 Fault model and data

The source rupture process of the largest aftershock is estimated by the same approach presented for the mainshock. The length and width of the fault plane are assumed to be 8 km and 8 km, respectively. According to the moment tensor solution by the F-net, the strike and dip of the fault plane are assumed to be 132° and 90°, respectively. The rupture starting point is fixed at the hypocenter location (33.67°N, 130.29°E, 13 km) determined by the ISV, Kyushu University. The fault plane is divided into 64 subfaults of 1 km × 1 km. The temporal slip history at each subfault is expressed by a series of 6 smoothed ramp functions, which has the rise time of 0.6 s, separated by 0.3 s.

Integrated ground velocities are bandpass filtered with a Chebyshev filter between 0.1 and 1.5 Hz. We inverted 6 s of the S-wave portion from 1 s before the S-wave arrival. The underground structure model to calculate Green's functions is the same for the mainshock modeling.

3.2 Result and discussions

Figure 6 shows the final slip distribution on the fault surface estimated by the waveform inversion. The rupture front propagation velocity, which triggers the rupture of the first time window, was selected to be 2.6 km/s. The rupture velocity was not constrained well because of its small spatial extent. As in the case of the mainshock, the rupture propagated to the southeastward. The northwest of the hypocenter had almost no slip on the fault. Figure 7 shows the comparison between observed and synthesized ground velocities in 0.1–1.5 Hz. The synthesized waveforms fit the observed ones fairly well. Figure 8 shows the moment rate functions at each subfault. The asperity was located in the vicinity of the hypocenter. The temporal rupture history was also rather simple, and the duration of source time function at each subfault is approximately 1 s on the asperity. The total seismic moment was obtained to be 2.81×10^{17} Nm (M_W5.6).

Figure 9 shows the spatial slip distributions of the mainshock and the largest aftershock. The rupture area of the largest aftershock and that of the mainshock do not overlap

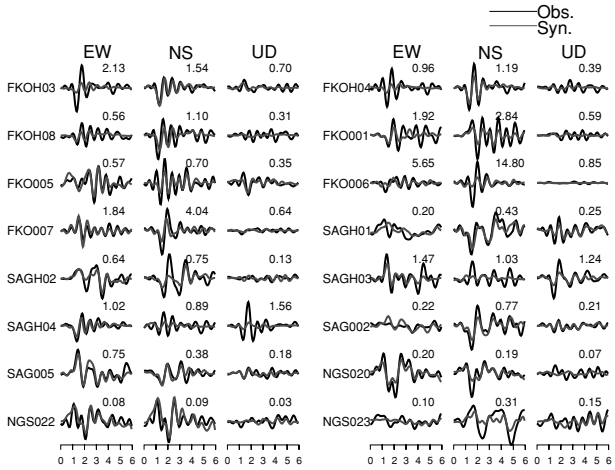

Fig. 7. Comparison between observed (black traces) and synthesized (gray traces) velocity waveforms of the largest aftershock. The maximum amplitude of each component of observed waveforms are shown above each trace in cm/s. The horizontal axis is time (s).

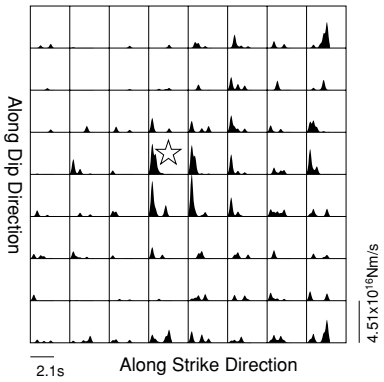

Fig. 8. Moment rate functions of each subfault of the largest aftershock. The open star indicates the hypocenter.

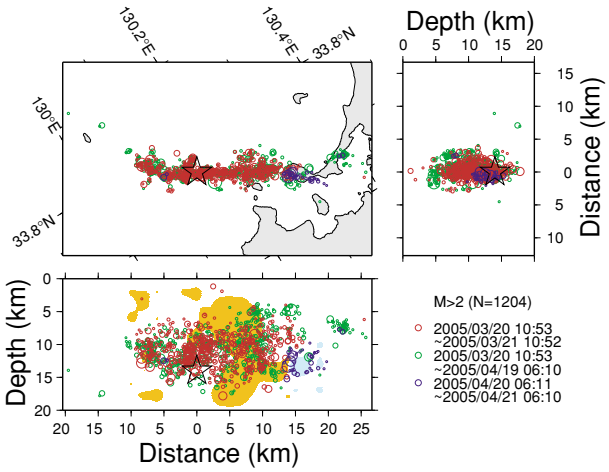

Fig. 9. Map showing hypocenters of aftershocks whose magnitude are larger than 2.0. The open circles are the hypocenters of aftershocks determined by the JMA. The colors of circles depend on the periods. Vertical section along the strike direction of the mainshock (N122°E) with the large slip area obtained by the kinematic waveform inversion of the mainshock and the largest aftershock is also shown in the bottom figure. The area in which the slip is larger than 0.8 m is colored orange for the mainshock, and the area in which the slip is larger than 0.2 m is colored light blue for the largest aftershock. The open star indicates the epicenter of the mainshock used in this study.

each other. Before the largest aftershock on April 20, few aftershocks occurred arround the hypocenter of this event. The strike of the spatial series of aftershocks which occured after the largest aftershock is slightly differs from that of aftershocks before the largest aftershock. The spatial and temporal pattern of aftershock distributions suggests that the largest aftershock might rupture the area in which the mainshock did not rupture.

4. Three-Dimensional Ground Motion Simulation

4.1 Ground motion simulation using the finite difference method

To see the spatial variation of strong ground motions in the near-source region, a three-dimensional ground motion simulation is carried out with the use of the finite difference method using staggered grids with nonuniform spacing developed by Pitarka (1999). The source model obtained above is adopted to simulate the ground motion generation on the fault. A three-dimensional underground structure model is constructed by manually digitizing the gravity basement depth contour map, which was produced by Komazawa (2005) from gravity anomalies. Figure 10 shows the depth of the bedrock surface with the shear-wave velocity (V_S) of 2850 m/s. Three sedimentary layers (V_S = 600, 1100, 1700 m/s) are assumed above the bedrock. Material parameters assumed for this layered underground structure model basically follow that of Nakamichi and Kawase (2002), and those parameters of each layer are listed in Table 1. h is the depth of the bedrock surface shown in Fig. 10. The dimensions of the model space are 701, 701, and 208 in the x, y, and z directions. The grid spacing is set to 0.1 km in the x and y directions and 0.1 km and 0.2 km in the z direction in the depth intervals of 0 to 2 km and 2 to 40 km, respectively. The time step is 0.00682 s, the total number of time steps is 2933, and the duration of synthetic waveforms is 20 s. The target frequency range of the calculation is up to 1.0 Hz. The simulated distribution of maximum horizontal velocity at surface is shown in Fig. 11. The area where large ground motion was expected from the simulation extended to the southeastward from the fault because of the relatively deep basin structure in the center of Fukuoka City as well as the forward directivity effect of the fault rupture. Genkai Island and Shikanoshima Island are located in the area with large ground motion above the fault. The localized area with relatively large ground motions were also expected at the northwest of the hypocenter and around the hypocenter. Those are mainly controlled by the temporal fault rupture process.

4.2 Discussion

Figure 12 shows the distribution of strong motion stations in Fukuoka City by the K-NET, the Japan Meteorological Agency (JMA), and Fukuoka City Government. Recently, the JMA and local governments of all over Japan have deployed seismic intensity and strong ground motion observation system (e.g., Nishimae, 2004). In Fukuoka City, strong ground motions during the mainshock were densely

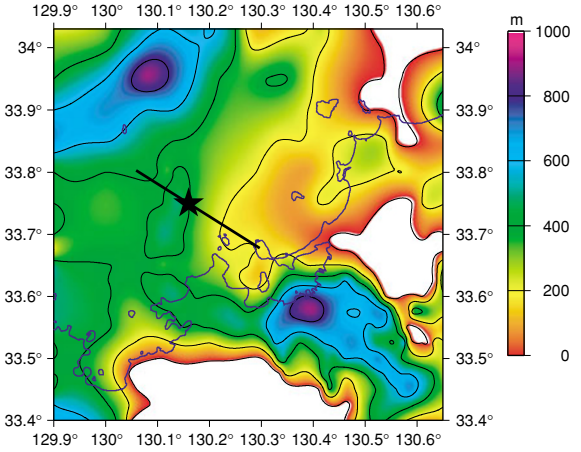

Fig. 10. Depth contour map showing the surface of the bedrock with the shear-wave velocity of 2850 m/s. The interval of contours is 200 m.

Table 1. Model parameters of each layer of the underground structure model used in the finite difference calculation.

Depth (m)	V_P (m/s)	V_S (m/s)	ρ (kg/m^3)	Q
0	1900	600	1900	50
0.09 h	2600	1100	2100	100
0.38 h	3500	1700	2300	150
h	5150	2850	2500	250
2000	5500	3200	2600	300
5000	6000	3460	2700	350
18000	6700	3870	2800	400

h is the depth of the bedrock surface shown in Fig. 10.

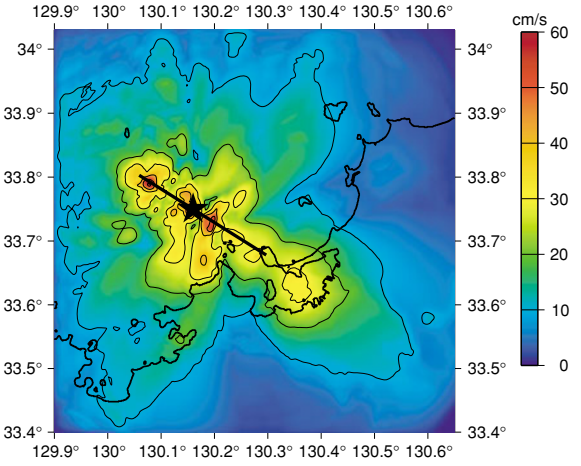

Fig. 11. Spatial distribution of slimulated maximum horizontal velocity at surface. The interval of contours is 10 cm/s.

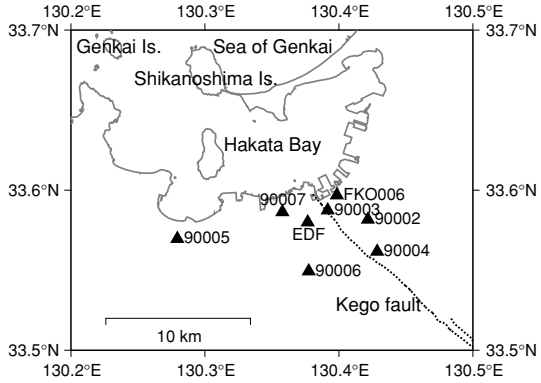

Fig. 12. Map showing the locations of strong motion stations in Fukuoka City. The station FKO006 belongs to the K-NET. The station EDF belongs to the JMA. The stations 90002–90007 were deployed by Fukuoka City Government. The broken line indicates the surface trace of the Kego fault (Nakata and Imaizumi, 2002).

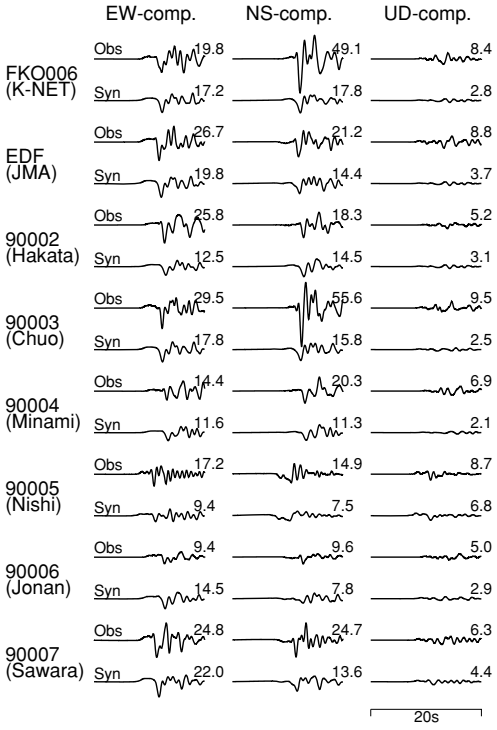

Fig. 13. Comparison of observed ground velocities with synthetic ones at stations in Fukuoka City. All traces are bandpass filtered between 0.05–1 Hz. Top and bottom traces for each station show the observed and synthetic waveforms, respectively. The peak ground velocity of each trace is shown at above each trace in cm/s.

recorded by these organizations. Figure 13 shows the comparison between observed and synthetic ground velocities (0.05–1 Hz) at the stations of the K-NET, the JMA, and Fukuoka City Government. Synthetic waveforms fit observed ones fairly well except several components. The observed amplitude of NS components at FKO006 and 90003 are exceptionally large compared with those at other stations. The simulation result could not succeed to reproduce the large amplitude of these components.

As shown in Fig. 12, the Kego fault runs through the central part of Fukuoka City (e.g., Nakata and Imaizumi, 2002; Oniki, 1996; The Research Group for Active Faults of Japan, 1991). Several studies reported that the depth of Quaternary deposits accumulated on the northeast side of the Kego fault are deeper than that on the southwest side (e.g., Karakida *et al.*, 1994; Nakamichi and Kawase, 2002; Oniki, 1996). The maximum thickness of Quaternary deposits along the Kego fault is approximately 60 m. Since the assumed shear-wave velocity at the surface in Table 1 is 600 m/s that corresponds to Paleogene sandstone, the Quaternary deposit was not included in this simulation. It

should cause the underestimation of synthetic ground velocities. Moreover, the horizontal irregularity of the bedrock structure caused by the Kego fault is not explicitly considered in our three-dimensional structure model, because the model is based on the gravity data and rather smooth. Such a lateral irregurarity causes the localized amplification along the fault trace in some case (e.g., Kawase, 1996; Pitarka *et al*., 1998). The mismatches of synthetic and observed ground velocities mentined above are found only at stations located at northeast side of the Kego fault. These mismatched might be attributed to the insufficient modeling with lack of the Quaternary deposits and the complex subsurface structure. More detailed modeling of the underground structure in Fukuoka City would be necessary to improve the propagation and amplification characteristics inside the basin.

5. Conclusions

The source rupture models of the 2005 West Off Fukuoka Prefecture earthquake and its largest aftershock were estimated by the kinematic waveform inversion of strong motion seismograms. The rupture area of the mainshock and that of the largest aftershock do not overlap each other. The ruptures of both events mainly propagated to the southeast direction from the hypocenters, and the asperity of the mainshock was observed at southeast of the hypocenter, and relatively smaller slip was observed in the vicinity of the hypocenter.

The forward simulation of the ground motions in the near-source region by the finite difference method showed that larger ground velocities were expected in Genkai Island, Shikanoshima Island, and the central district of Fukuoka City compared to other region. The feature and duration of the synthetic ground velocities in Fukuoka City matched the observed ones fairly well. However, absolute amplitude of the NS components of the synthetic ground velocities at several stations located at the footwall side of the Kego fault were underestimated compared with observed amplitudes. This underestimation would be caused by the insufficient modeling of complex subsurface structure in this area.

Acknowledgments. We are deeply indebted to the K-NET and the KiK-net operated by the NIED for releasing the strong motion data. We are also grateful to the JMA, Fukuoka City Government, and Prof. Hiroshi Kawase at Kyushu University for strong motion data recorded in Fukuoka City. We used the hypocenter information of the ISV, Kyushu University and the JMA, and the moment tensor catalog of the F-net by the NIED. We would like to thank Dr. Haruko Sekiguchi and Dr. Arben Pitarka for kindly allowing us to use their original codes. This work has used 'Active Fault Shape File' from Nakata and Imaizumi (2002) (product serial number: DAFM1483). The Generic Mapping Tools (Wessel and Smith, 1998) was used to draw all the figures in this paper. The comments from Prof. Hiroshi Takenaka and Dr. Alessio Piatanesi were helpful in improving the manuscript. This study is partially supported by Grant-in-Aid for Special Purposes (17800001, PI. Prof. Kawase, Kyushu Univ.) and the Special Project for Earthquake Disaster Mitigation in Urban Areas from the Ministry of Education, Culture, Sports, Science, and Technology, Japan.

References

Akaike, H., Likelihood and the Bayes procedure, in *Bayesian Statistics*, edited by J. M. Bernardo, M. H. DeGroot, D. V. Lindley, and A. F. M. Smith, pp. 143–166, University Press, Valencia, Spain, 1980.

Aoi, S., K. Obara, S. Hori, K. Kasahara, and Y. Okada, New Japanese uphole/downhole strong-motion observation network: KiK-net, *Seism. Res. Lett*., **72**, 239, 2001.

Bouchon, M., A simple method to calculate Green's functions for elastic layered media, *Bull. Seism. Soc. Am*., **71**, 959–971, 1981.

Geller, R. J., Scaling relations for earthquake source parameters and magnitudes, *Bull. Seism. Soc. Am*., **71**, 1501–1523, 1976.

Hartzell, S. H. and T. H. Heaton, Inversion of strong ground motion and teleseismic waveform data for the fault rupture history of the 1979 Imperial Valley, Carifornia, earthquake, *Bull. Seism. Soc. Am*., **73**, 1553–1583, 1983.

Horikawa, H., Rupture process of the 2005 West Off Fukuoka Prefecture, Japan, earthquake, *Earth Planets Space*, **58**, this issue, 87–92, 2006.

Karakida, Y., S. Tomita, S. Shimoyama, and K. Chijiwa, *Geology of the Fukuoka District*, with Geological Sheet Map at 1:50,000, 192 pp., Geological Survey of Japan, Tsukuba, 1994 (in Japanese with English summary).

Kawase, H., The cause of the damage belt in Kobe: "The basin-edge effect," constructive interference of the direct S-wave with the basin-induced diffracted/Rayleigh waves, *Seism. Res. Lett*., **67**(5), 25–35, 1996.

Kennett, B. L. N. and N. J. Kerry, Seismic waves in a stratified half space, *Geophys. J. Roy. Astr. Soc*., **57**, 557–583, 1979.

Kinoshita, S., Kyoshin-net (K-NET), *Seism. Res. Lett*., **69**, 309–332, 1998.

Kobayashi, R., S. Miyazaki, and K. Koketsu, Source processes of the 2005 West Off Fukuoka Prefecture earthquake and its largest aftershock inferred from strong motion and 1-Hz GPS data, *Earth Planets Space*, **58**, this issue, 57–62, 2006.

Komazawa, M., Gravity field around the source region of the 2005 west off Fukuoka earthquake, *Rep. Coord. Comm. Earthq. Pred*., **74**, 507–509, 2005 (in Japanese).

Lawson, C. L. and R. J. Hanson, *Solving Least Squares Problems*, 340 pp., Prentice-Hall, New Jersey, 1974.

Nakamichi, S. and H. Kawase, Broadband strong motion simulation in Fukuoka City based on a three-dimensional basin structure and a hybrid method, *J. Struct. Constr. Eng., AIJ*, **560**, 83–91, 2002 (in Japanese with English abstract).

Nakata, T. and T. Imaizumi (eds.), *Digital Active Fault Map of Japan*, 60 pp. with 2 DVD-ROM, University of Tokyo Press, Tokyo, 2002 (in Japanese).

Nishimae, Y., Observation of seismic intensity and strong ground motion by Japan Meteorological Agency and local governments in Japan, *J. Jpn. Assoc. Earthq. Eng*., **4**, 3 (Special Issue), 75–78, 2004.

Oniki, F., Precise location and subsurface features of the Kego fault in Fukuoka-city, north Kyushu, Japan, *Active Fault Research*, **15**, 37–45, 1996 (in Japanese with English abstract).

Pitarka, A., 3D elastic finite-difference modeling of seismic motion using staggered grids with nonuniform spacing, *Bull. Seism. Soc. Am*., **89**, 54–68, 1999.

Pitarka, A., K. Irikura, T. Iwata, and H. Sekiguchi, Three-dimensional simulation of the near-fault ground motion for the 1995 Hyogo-ken Nanbu (Kobe), Japan, earthquake, *Bull. Seism. Soc. Am*., **88**, 428–440, 1998.

Sekiguchi, H., S. Aoi, R. Honda, N. Morikawa, T. Kunugi, and H. Fujiwara, Rupture process of the 2005 West Off Fukuoka Prefecture earthquake obtained from strong motion data of K-NET and KiK-net, *Earth Planets Space*, **58**, this issue, 37–43, 2006.

Sekiguchi, H., K. Irikura, and T. Iwata, Fault geometry in the rupture termination of the 1995 Hyogo-ken Nanbu earthquake, *Bull. Seism. Soc. Am*., **90**, 117–133, 2000.

Seno, T., Syntheses of the regional stress fields of the Japanese islands, *Island Arc*, **8**, 66–79, 1999.

Takenaka, H., T. Nakamura, Y. Yamamoto, G. Toyokuni, and H. Kawase, Precise location of the fault plane and the onset of the main rupture of the 2005 West Off Fukuoka Prefecture earthquake, *Earth Planets Space*, **58**, this issue, 75–80, 2006.

The Research Group for Active Faults of Japan, *Active Faults in Japan: Sheet Maps and Inventories (Revised Edition)*, 437 pp., University of Tokyo Press, Tokyo, 1991 (in Japanese with English summary).

Wessel, P. and W. H. F. Smith, New, improved version of Generic Mapping Tools released, *Eos Trans. Am. Geophys. Union*, **79**, 579, 1998.

K. Asano (e-mail: k-asano@egmdpri01.dpri.kyoto-u.ac.jp) and T. Iwata